ICIC Express Letters
Volume **18**, Number **2**, February **2024**

ICIC International ©2024 ISSN 1881-803X
pp. 151–157

GENERATION OF ABSTRACT-PAINTING IMAGES USING POISSON DISTRIBUTION AND ENTROPY

Toru Hiraoka[1] and Takeshi Kameyam[2]

[1]Department of Information Systems
University of Nagasaki
1-1-1, Manabino, Nagayo-chou, Nishisonogi-gun, Nagasaki-ken 851-2195, Japan
hiraoka@sun.ac.jp

[2]Nagasaki Prefectural Government
3-1, Onoue-machi, Nagasaki-shi, Nagasaki-ken 850-0058, Japan
t.kameyama@pref.nagasaki.lg.jp

Received April 2023; accepted July 2023

Abstract. *In the technology called non-photorealistic rendering (NPR), which pursues artistic expressions and visual appeal without sticking to realistic expressions, NPR with various expressions is required. Therefore, we propose an NPR method for automatically generating abstract-painting images from photographic images. Abstract painting is an art that bright paints are randomly painted and mixed colors are beautiful. The proposed method is executed by an iterative calculation using Poisson distribution and entropy. To verify the effectiveness of the proposed method, an experiment was conducted to visually confirm abstract-painting images generated by applying the proposed method to various photographic images. Additionally, an experiment was conducted to visually confirm the changes in abstract-painting patterns generated by changing the values of the parameters in the proposed method.*

Keywords: Non-photorealistic rendering, Abstract painting, Poisson distribution, Entropy, Automatic generation

1. **Introduction.** Many researches on non-photorealistic rendering (NPR) have been conducted so far [1, 2, 3, 4]. NPR is a computer graphics technology [5, 6] that generates non-photorealistic images that convey visual information more effectively and enhance artistry and entertainment by drawing with various enhancements and omissions such as paintings and illustrations. Further, when NPR is classified according to the input data, non-photorealistic images are automatically or semi-automatically converted from images, videos and three-dimensional data.

In this paper, we focus on NPR that automatically converts non-photorealistic images from photographic images. Additionally, we consider NPR to generate abstract-painting images. Abstract paintings are an art that bright paints are randomly painted and mixed colors are beautiful. In general, abstract paintings make it difficult to see what is drawn. Abstract-painting images preserve the edges of photographic images and makes it easier to recall photographic images. Similar to the proposed method, NPR methods have been proposed for generating pop-art images [7] and thermographic images [8] that are colorful, preserve the edges and can recall photographic images. Pop-art images are generated by image processing [9, 10] using binomial distribution, and thermographic images are generated by an iterative processing using inverse filter [11] and smoothing filter with swapping between RGB. Abstract-painting images are non-photorealistic images with textures different from those of pop-art images and thermographic images.

DOI: 10.24507/icicel.18.02.151

The proposed method is executed by an iterative calculation using Poisson distribution and entropy. To verify the effectiveness of the proposed method, an experiment is conducted to visually confirm abstract-painting images generated by applying the proposed method to various photographic images. Additionally, an experiment is conducted to visually confirm the changes in abstract-painting patterns generated by changing the values of the parameters in the proposed method.

This paper is organized as follows: the second section describes the proposed method for automatically generating abstract-painting images from photographic images, the third section shows experimental results and reveals the effectiveness of the proposed method, and the conclusion of this paper is given in the fourth section.

2. Proposed Method.

The proposed method is executed in two steps: Step 1 calculates entropy using Poisson distribution, and Step 2 uses entropy to convert photographic images. Since Poisson distribution is particularly suitable for modeling the occurrence frequency of rare events, the use of Poisson distribution in the proposed method allows us to consider the effects of characteristic regions in photographic images that occur infrequently. Abstract-painting images are generated by iterating through Steps 1 and 2. A flow chart of the proposed method is shown in Figure 1.

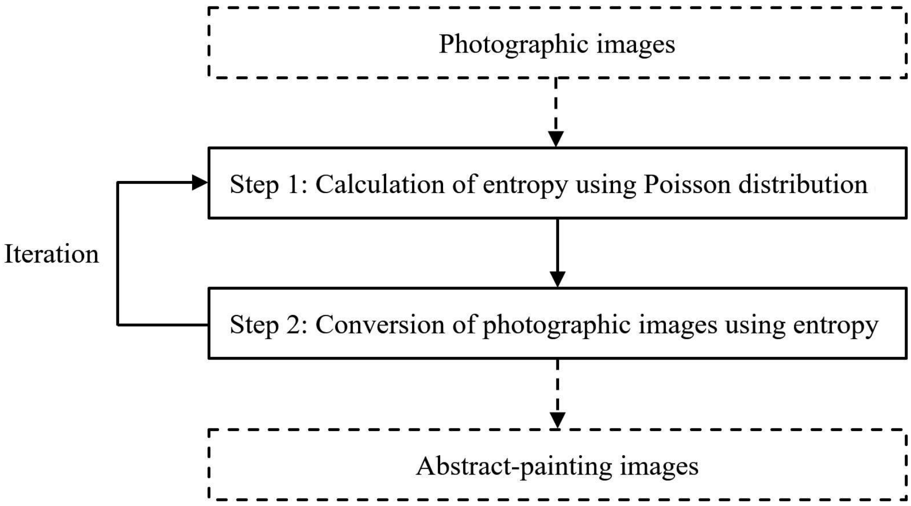

FIGURE 1. Flow chart of the proposed method

Details of the procedure in Figure 1 are explained below.

Step 0: The input pixel values (R, G, B) on spatial coordinates (i, j) are defined as $f_{R,i,j}$, $f_{G,i,j}$ and $f_{B,i,j}$, respectively. The pixel values $f_{R,i,j}$, $f_{G,i,j}$ and $f_{B,i,j}$ have value of U gradations from 0 to $U-1$. The pixel values of the image at the t-th iteration number are defined as $f^{(t)}_{R,i,j}$, $f^{(t)}_{G,i,j}$ and $f^{(t)}_{B,i,j}$, where $f^{(0)}_{R,i,j} = f_{R,i,j}$, $f^{(0)}_{G,i,j} = f_{G,i,j}$ and $f^{(0)}_{B,i,j} = f_{B,i,j}$.

Step 1: The range of pixel values is divided into M divisions, and the pixel values $f^{(t)}_{R,i,j}$, $f^{(t)}_{G,i,j}$ and $f^{(t)}_{B,i,j}$ are assigned to the division, respectively. The assigned divisions $d^{(t)}_{R,i,j}$, $d^{(t)}_{G,i,j}$ and $d^{(t)}_{B,i,j}$ have integer values from 0 to $M-1$, and are calculated by the following equations, respectively.

$$d^{(t)}_{R,i,j} = round\left(\frac{af^{(t-1)}_{R,i,j} + f^{(t-1)}_{G,i,j} + f^{(t-1)}_{B,i,j}}{(a+2)M}\right) \tag{1}$$

$$d^{(t)}_{G,i,j} = round\left(\frac{f^{(t-1)}_{R,i,j} + af^{(t-1)}_{G,i,j} + f^{(t-1)}_{B,i,j}}{(a+2)M}\right) \tag{2}$$

$$d_{B,i,j}^{(t)} = round\left(\frac{f_{R,i,j}^{(t-1)} + f_{G,i,j}^{(t-1)} + af_{B,i,j}^{(t-1)}}{(a+2)M}\right) \tag{3}$$

where a is a positive constant and $round()$ is a function that truncates after the decimal point. At the assigned divisions $d_{R,i,j}^{(t)}$, $d_{G,i,j}^{(t)}$ and $d_{B,i,j}^{(t)}$, the probabilities $p_{R,i,j,m}^{(t)}$, $p_{G,i,j,m}^{(t)}$ and $p_{B,i,j,m}^{(t)}$ that the division m $(= 0, 1, \ldots, M-1)$ appears within $\pm W$ around the spatial coordinate (i, j) are calculated, respectively, where W is a positive constant representing the window size.

When m is less than $M-1$, the Poisson distributions $P_{R,i,j,m}^{(t)}$, $P_{G,i,j,m}^{(t)}$ and $P_{B,i,j,m}^{(t)}$ are calculated by the following equations, respectively.

$$P_{R,i,j,m}^{(t)} = \frac{\left(\frac{1}{p_{R,i,j,m}^{(t)}}\right)^m e^{-\frac{1}{p_{R,i,j,m}^{(t)}}}}{m!} \tag{4}$$

$$P_{G,i,j,m}^{(t)} = \frac{\left(\frac{1}{p_{G,i,j,m}^{(t)}}\right)^m e^{-\frac{1}{p_{G,i,j,m}^{(t)}}}}{m!} \tag{5}$$

$$P_{B,i,j,m}^{(t)} = \frac{\left(\frac{1}{p_{B,i,j,m}^{(t)}}\right)^m e^{-\frac{1}{p_{B,i,j,m}^{(t)}}}}{m!} \tag{6}$$

The Poisson distributions $P_{R,i,j,M-1}^{(t)}$, $P_{G,i,j,M-1}^{(t)}$ and $P_{B,i,j,M-1}^{(t)}$ are calculated by the following equations, respectively.

$$P_{R,i,j,M-1}^{(t)} = 1 - \sum_{m=0}^{M-2} P_{R,i,j,m}^{(t)} \tag{7}$$

$$P_{G,i,j,M-1}^{(t)} = 1 - \sum_{m=0}^{M-2} P_{G,i,j,m}^{(t)} \tag{8}$$

$$P_{B,i,j,M-1}^{(t)} = 1 - \sum_{m=0}^{M-2} P_{B,i,j,m}^{(t)} \tag{9}$$

The entropies $E_{R,i,j}^{(t)}$, $E_{G,i,j}^{(t)}$ and $E_{B,i,j}^{(t)}$ are calculated by the following equations using the Poisson distributions $P_{R,i,j,m}^{(t)}$, $P_{G,i,j,m}^{(t)}$ and $P_{B,i,j,m}^{(t)}$, respectively.

$$E_{R,i,j}^{(t)} = -\sum_{m=0}^{M-1} P_{R,i,j,m}^{(t)} \log_2 P_{R,i,j,m}^{(t)} \tag{10}$$

$$E_{G,i,j}^{(t)} = -\sum_{m=0}^{M-1} P_{G,i,j,m}^{(t)} \log_2 P_{G,i,j,m}^{(t)} \tag{11}$$

$$E_{B,i,j}^{(t)} = -\sum_{m=0}^{M-1} P_{B,i,j,m}^{(t)} \log_2 P_{B,i,j,m}^{(t)} \tag{12}$$

The average values $E_{R,i,j,ave}^{(t)}$, $E_{G,i,j,ave}^{(t)}$ and $E_{B,i,j,ave}^{(t)}$ of the entropies $E_{R,i,j}^{(t)}$, $E_{G,i,j}^{(t)}$ and $E_{B,i,j}^{(t)}$ are calculated, respectively. Additionally, the standard deviations $E_{R,i,j,sta}^{(t)}$, $E_{G,i,j,sta}^{(t)}$ and $E_{B,i,j,sta}^{(t)}$ of the entropies $E_{R,i,j}^{(t)}$, $E_{G,i,j}^{(t)}$ and $E_{B,i,j}^{(t)}$ are calculated, respectively.

Step 2: The pixel values $f_{R,i,j}^{(t)}$, $f_{G,i,j}^{(t)}$ and $f_{B,i,j}^{(t)}$ are calculated by the following equations using the entropies $E_{R,i,j}^{(t)}$, $E_{G,i,j}^{(t)}$ and $E_{B,i,j}^{(t)}$, respectively.

$$f_{R,i,j}^{(t)} = \begin{cases} f_{i,j} + \dfrac{(U-1)\left(E_{R,i,j}^{(t)} - E_{R,i,j,ave}^{(t)}\right)}{2E_{R,i,j,sta}^{(t)}} & (t\%2=0) \\ f_{i,j} - \dfrac{(U-1)\left(E_{R,i,j}^{(t)} - E_{R,i,j,ave}^{(t)}\right)}{2E_{R,i,j,sta}^{(t)}} & (t\%2=1) \end{cases} \tag{13}$$

$$f_{G,i,j}^{(t)} = \begin{cases} f_{i,j} + \dfrac{(U-1)\left(E_{G,i,j}^{(t)} - E_{G,i,j,ave}^{(t)}\right)}{2E_{G,i,j,sta}^{(t)}} & (t\%2=0) \\ f_{i,j} - \dfrac{(U-1)\left(E_{G,i,j}^{(t)} - E_{G,i,j,ave}^{(t)}\right)}{2E_{G,i,j,sta}^{(t)}} & (t\%2=1) \end{cases} \tag{14}$$

$$f_{B,i,j}^{(t)} = \begin{cases} f_{i,j} + \dfrac{(U-1)\left(E_{B,i,j}^{(t)} - E_{B,i,j,ave}^{(t)}\right)}{2E_{B,i,j,sta}^{(t)}} & (t\%2=0) \\ f_{i,j} - \dfrac{(U-1)\left(E_{B,i,j}^{(t)} - E_{B,i,j,ave}^{(t)}\right)}{2E_{B,i,j,sta}^{(t)}} & (t\%2=1) \end{cases} \tag{15}$$

where the notation % represents a remainder operation. When the pixel values $f_{R,i,j}^{(t)}$, $f_{G,i,j}^{(t)}$ and $f_{B,i,j}^{(t)}$ are less than 0, $f_{R,i,j}^{(t)}$, $f_{G,i,j}^{(t)}$ and $f_{B,i,j}^{(t)}$ must be set to 0, respectively. When the pixel values $f_{R,i,j}^{(t)}$, $f_{G,i,j}^{(t)}$ and $f_{B,i,j}^{(t)}$ are greater than $U-1$, $f_{R,i,j}^{(t)}$, $f_{G,i,j}^{(t)}$ and $f_{B,i,j}^{(t)}$ must be set to $U-1$, respectively.

An abstract-painting image is obtained after Steps 1 and 2 of T times iteration.

3. Experiments.

We conducted two experiments: the first experiment was to visually confirm the changes in abstract-painting patterns generated by changing the values of the parameters in the proposed method, and the second experiment was to apply the proposed method to various photographic images. The first experiment used Pepper image shown in Figure 2, and the second experiment used 3 photographic images shown in Figure 3. All photographic images used in the experiments were $512*512$ pixels and 256 gradations. Unless otherwise noted, the values of the parameters M, a, W and T were set to 16, 10, 8 and 30, respectively.

FIGURE 2. Pepper image

FIGURE 3. Various photographic images

3.1. **Experiment with changing parameters.** Abstract-painting images generated by changing the value of the parameter M were visually confirmed using Pepper image. The value of M was set to 4, 16 and 32. The results of the experiment are shown in Figure 4. As the value of M was larger, abstract-painting images had more abstract-painting patterns.

(a) $M = 4$ (b) $M = 16$ (c) $M = 32$

FIGURE 4. Abstract-painting images in the case of $M = 4$, 16 and 32

Abstract-painting images generated by changing the value of the parameter a were visually confirmed using Pepper image. The value of a was set to 5, 10 and 15. The results of the experiment are shown in Figure 5. As the value of a was larger, abstract-painting images had more abstract-painting patterns and abstract-painting patterns were expressed more clearly.

(a) $a = 5$ (b) $a = 10$ (c) $a = 15$

FIGURE 5. Abstract-painting images in the case of $a = 5$, 10 and 15

Abstract-painting images generated by changing the value of the parameter W were visually confirmed using Pepper image. The value of W was set to 4, 8 and 12. The results of the experiment are shown in Figure 6. As the value of W was larger, the size of abstract-painting patterns was expressed larger.

(a) $W = 4$ (b) $W = 8$ (c) $W = 12$

FIGURE 6. Abstract-painting images in the case of $W = 4$, 8 and 12

Abstract-painting images generated by changing the value of the parameter T were visually confirmed using Pepper image. The value of T was set to 10, 20 and 30. The results of the experiment are shown in Figure 7. As the value of T was larger, abstract-painting patterns were expressed more clearly and finely.

(a) $T = 10$ (b) $T = 20$ (c) $T = 30$

FIGURE 7. Abstract-painting images in the case of $T = 10$, 20 and 30

3.2. **Experiment using various photographic images.** The proposed method was applied to 3 photographic images shown in Figure 3. The results of the experiment are shown in Figure 8. All abstract-painting images were expressed by abstract-painting patterns that were randomly and colorfully expressed. Additionally, all abstract-painting images could preserve the edges of photographic images.

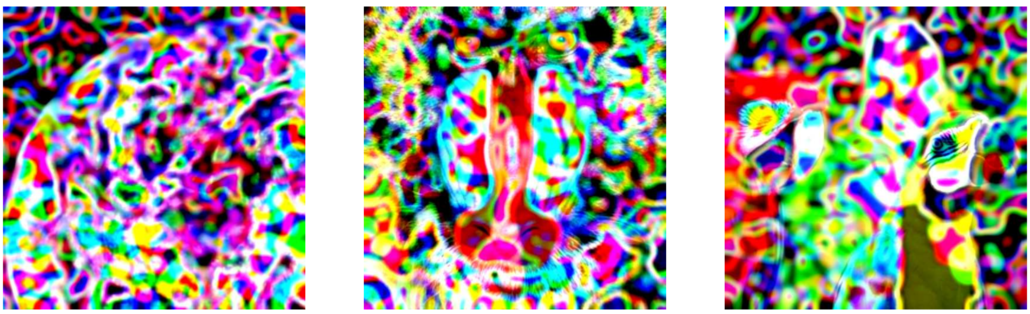

FIGURE 8. Various abstract-painting images

4. **Conclusions.** We proposed an NPR method to automatically generate abstract-painting images from photographic images. The proposed method was executed by an iterative calculation using Poisson distribution and entropy. To verify the effectiveness of the proposed method, an experiment was conducted to visually confirm abstract-painting images

generated by applying the proposed method to various photographic images. Additionally, an experiment was conducted to visually confirm the changes in abstract-painting patterns generated by changing the values of the parameters in the proposed method. As a result of the experiments, it was found that the proposed method can preserve the edges of photographic images. It was also found that the width and number of abstract-painting patterns can be changed by changing the values of the parameters.

The future task is to apply the proposed method to videos and three-dimensional data.

Acknowledgment. This work was supported by JSPS KAKENHI Grant Number JP23K 11727 and The Telecommunications Advancement Foundation Grant.

REFERENCES

[1] J. Correia, L. Vieira, N. Rodriguez-Fernandez, J. Romero and P. Machado, Evolving image enhancement pipelines, *Artificial Intelligence in Music, Sound, Art and Design*, pp.82-97, 2021.
[2] P. L. Rosin, Y. K. Lai, D. Mould, R. Yi, I. Berger, L. Doyle, S. Lee, C. Li, Y. J. Liu, A. Semmo, A. Shamir, M. Son and H. Winnemoller, NPRportrait 1.0: A three-level benchmark for nonphotorealistic rendering of portraits, *Computational Visual Media*, vol.8, no.3, pp.445-465, 2022.
[3] Y. Zhao, D. Ren, Y. Chen, W. Jia, R. Wang and X. Liu, Cartoon image processing: A survey, *International Journal of Computer Vision*, vol.130, no.11, pp.2733-2769, 2022.
[4] W. Ye, X. Zhu and Y. Liu, Multi-semantic preserving neural style transfer based on Y channel information of image, *The Visual Computer*, vol.39, no.2, pp.609-623, 2023.
[5] D. Koschier, J. Bender, B. Solenthaler and M. Teschner, A survey on SPH methods in computer graphics, *Computer Graphics Forum*, vol.41, no.2, pp.737-760, 2022.
[6] F. Weidner, G. Boettcher, S. A. Arboleda, C. Diao, L. Sinani, C. Kunert, C. Gerhardt, W. Broll and A. Raake, A systematic review on the visualization of avatars and agents in AR & VR displayed using head-mounted displays, *IEEE Transactions on Visualization and Computer Graphics*, vol.29, no.5, pp.2596-2606, 2023.
[7] T. Hiraoka, Generation of pop art-like images using binomial distribution, *ICIC Express Letters*, vol.14, no.3, pp.227-233, 2020.
[8] T. Hiraoka, Generation of edge-preserving thermographic images using inverse filter and smoothing filter with swapping between RGB, *ICIC Express Letters*, vol.15, no.7, pp.719-724, 2021.
[9] K. Ogura, N. Shigei and H. Miyajima, Robust person tracking by pan-tilt camera with low-cost single board computer, *ICIC Express Letters*, vol.16, no.4, pp.381-389, 2022.
[10] H. Chen and Z.-M. Lu, Dynamic smoke detection by eliminating static targets in video, *International Journal of Innovative Computing, Information and Control*, vol.19, no.2, pp.355-364, 2023.
[11] Z. Yu and K. Urahama, Iterative method for inverse nonlinear image processing, *IEICE Transactions on Fundamentals*, vol.E97-A, no.2, pp.719-721, 2014.